ORIGINAL ARTICLE

MOLECULAR ECOLOGY WILEY

Extensive introgression at late stages of species formation: Insights from grasshopper hybrid zones

Linda Hagberg[1] | Enrique Celemín[1,2] | Iker Irisarri[3,4] | Oliver Hawlitschek[5,6] | José L. Bella[7,8] | Tamí Mott[9] | Ricardo J. Pereira[1]

[1]Division of Evolutionary Biology, Faculty of Biology II, Ludwig-Maximilians-Universität München, Planegg-Martinsried, Germany

[2]Unit of Evolutionary Biology/Systematic Zoology, Institute of Biochemistry and Biology, Universität Potsdam, Potsdam, Germany

[3]Institute for Microbiology and Genetics, Department of Applied Bioinformatics, University of Goettingen, Göttingen, Germany

[4]Campus Institute Data Science (CIDAS), Göttingen, Germany

[5]Leibniz Institute for the Analysis of Biodiversity Change, Zoological Museum, Hamburg, Germany

[6]Zoologische Staatssammlung (SNSB-ZSM), Munich, Germany

[7]Departamento de Biología (Genética), Facultad de Ciencias, Universidad Autónoma de Madrid, Madrid, Spain

[8]Centro de Investigación en Biodiversidad y Cambio Global (CIBC-UAM), Universidad Autónoma de Madrid, Madrid, Spain

[9]Instituto de Ciências Biológicas e da Saúde, Universidade Federal de Alagoas, Maceió, Brazil

Correspondence
Ricardo J. Pereira, Division of Evolutionary Biology, Faculty of Biology II, Ludwig-Maximilians-Universität München, Grosshaderner Strasse 2, 82152 Planegg-Martinsried, Germany.
Email: ricardojn.pereira@gmail.com

Funding information
Deutsche Forschungsgemeinschaft, Grant/Award Number: HA7255/2-1; H2020 Marie Skłodowska-Curie Actions, Grant/Award Number: 658706; Ministerio de Ciencia, Innovación y Universidades, Grant/Award Number: PID2019-104952GB-I00/AEI/10.13039/501100011033

Handling Editor: Sean Schoville

Abstract

The process of species formation is characterized by the accumulation of multiple reproductive barriers. The evolution of hybrid male sterility, or Haldane's rule, typically characterizes later stages of species formation, when reproductive isolation is strongest. Yet, understanding how quickly reproductive barriers evolve and their consequences for maintaining genetic boundaries between emerging species remains a challenging task because it requires studying taxa that hybridize in nature. Here, we address these questions using the meadow grasshopper *Pseudochorthippus parallelus*, where populations that show multiple reproductive barriers, including hybrid male sterility, hybridize in two natural hybrid zones. Using mitochondrial data, we infer that such populations diverged some 100,000 years ago, at the beginning of the last glacial cycle in Europe. Nuclear data show that contractions at multiple glacial refugia, and post-glacial expansions have facilitated genetic differentiation between lineages that today interact in hybrid zones. We find extensive introgression throughout the sampled species range, irrespective of the current strength of reproductive isolation. Populations exhibiting hybrid male sterility in two hybrid zones show repeatable patterns of genomic differentiation, consistent with shared genomic constraints affecting ancestral divergence or with the role of those regions in reproductive isolation. Together, our results suggest that reproductive barriers that characterize late stages of species formation can evolve relatively quickly, particularly when associated with

strong demographic changes. Moreover, we show that such barriers persist in the face of extensive gene flow, allowing future studies to identify associated genomic regions.

KEYWORDS

Haldane's rule, hybridization, *Pseudochorthippus parallelus*, speciation, sterility

1 | INTRODUCTION

The process of species formation is characterized by the gradual accumulation of multiple reproductive barriers between diverging taxa, and of their underlying genetic incompatibilities. Nascent species can be isolated from one another by incompatible mating signals that prevent interbreeding (Naisbit et al., 2001), by incompatible ecological interactions that render hybrids unfit in either extrinsic parental habitat (Thompson et al., 2022), or by incompatible gene interactions that cause intrinsic hybrid dysfunction such as sterility or inviability (Masly & Presgraves, 2007). All of these incompatibilities can be generally explained by the Bateson (1909), Dobzhansky (1936) and Muller (1942) model, which states that mutations that are adaptive or nearly neutral in their own genomic background can be functionally incompatible with alleles that are present in a foreign genomic background (Presgraves, 2010). Incompatibilities causing hybrid sterility are characteristic of late stages of species formation (Bracewell et al., 2017) because they are thought to be irreversible (Sobel et al., 2010). Understanding how hybrid sterility evolves and how it restricts gene flow between emergent species remains an important task in evolutionary biology (Coughlan & Matute, 2020; Coyne, 2018; Payseur et al., 2018; Payseur & Rieseberg, 2016; Presgraves, 2018).

Although the process of species formation is notoriously idiosyncratic, the observation of pervasive patterns of reproductive isolation across species pairs suggests that generalities, or "rules" (Coyne & Orr, 1989), underlie species formation in all animals. "Haldane's rule" states that whenever a sex is absent, rare or sterile in a cross between two taxa, that sex is usually the heterogametic sex (Haldane, 1922). This empirical observation has been elucidated by laboratorial interspecific crosses showing that alleles involved in incompatibilities are generally recessive (Masly & Presgraves, 2007), so that their deleterious effects in hybrids are masked in the diploid chromosomes (i.e., autosomes and sexual chromosomes in the homogametic sex, XX females and ZZ males), but are exposed in the haploid sexual chromosomes in the heterogametic sex (i.e., XY and X0 males or ZW females). Most of the current knowledge on Haldane's rule stems from experimental crosses between highly divergent species, namely drosophilids (Masly & Presgraves, 2007; Payseur et al., 2018; Presgraves, 2018; Presgraves & Meiklejohn, 2021) that speciated between 4,000,000 and 300,000 years ago (Kliman et al., 2000; Wang & Hey, 1996). With some exceptions (Ebdon et al., 2021; Matute, 2010; Teeter et al., 2007), these species rarely hybridize in nature and laboratory hybrids are often lethal or inviable (Matute & Cooper, 2021). Thus, incompatibilities manifested

in these systems may have arisen after reproductive isolation has been established (Coyne, 2018; Matute, 2010), questioning their role in limiting gene flow between incipient species and hence in facilitating species formation.

Hybrid zones provide a direct insight into the phenotypes and underlying genes that maintain genetic barriers between emerging species, and that thus presumably facilitate species formation (Barton & Hewitt, 1985; Harrison, 1993). Hybrid zones are broadly defined as areas in which incipient species meet, mate, and produce at least some offspring of mixed ancestry (Harrison, 1990), and can be observed between recently diverged taxa, such as incipient species, subspecies, or even differentiated populations. Genetic boundaries between hybridising taxa can remain stable if selection against incompatible loci is strong enough to balance the homogenising effect of dispersal of parental individuals into the hybrid zone (i.e., tension zones; Barton & Hewitt, 1985). Unlike experimental hybridization that is necessarily limited to few generations of recombination, hybrid zones result from thousands of generations of recombination, reducing physical linkage among loci involved in early incompatibilities and neutral loci, and allowing for high resolution to map genes underlying reproductive isolation (Rieseberg et al., 2000). Moreover, incompatibilities expressed in hybrid zones are usually associated with mildly maladaptive phenotypes such as partial sterility (Nachman & Payseur, 2012; Nürnberger et al., 2016), instead of full sterility and inviability. Hybrid zones exhibiting the same reproductive barriers are particularly useful as they allow testing for replicated patterns of genomic differentiation linked to barriers to gene flow or to shared genomic constrains (Poelstra et al., 2014; Ravinet et al., 2016; Westram et al., 2021), thus offering insights into predictability of evolution at the gene level (Christin et al., 2010; Stern & Orgogozo, 2009).

The meadow grasshopper *Pseudochorthippus parallelus*, formerly known as *Chorthippus parallelus* (Defaut, 2012), is a suitable system to shed light on how late reproductive barriers, such as Haldane's rule evolve, and how they contribute to limiting gene flow between emerging species. Like most species in Europe (Hewitt, 2000), this species survived in isolated southern refugia in the Iberian, Italian and Balkan peninsulas, as permanent ice covered northern latitudes during the Pleistocene ice ages (>15,000 years ago; Butlin, 1998; Hewitt, 1993; Ivy-Ochs et al., 2008). Geographical isolation resulted in the formation of two subspecies, *P. p. erythropus* in Iberia and *P. p. parallelus* in the remaining peninsulas, which differ in morphology, behaviour, cytogenetics and molecular markers (Butlin & Hewitt, 1985; Butlin et al., 1991; Cooper et al., 1995; Gosálvez et al., 1988; Serrano et al., 1996). After the retraction of the ice coverage,

the two subspecies expanded and established a hybrid zone in the Pyrenees, when the ice last disappeared some 8000 years ago (Hewitt, 1993), which in this univoltine species (one generation per year) corresponds to 8,000 generations since the most recent secondary contact. About the same elevation and presumably at the same time in the Alps (Palacios et al., 2017), two evolutionary lineages assigned to the subspecies *P. p. parallelus* established a second hybrid zone (Cooper et al., 1995). Limited molecular data based on one mitochondrial and one nuclear gene (Korkmaz et al., 2014; Lunt et al., 1998) could not establish the phylogenetic relationships between these three lineages (Cooper et al., 1995), and thus it remains unclear when these taxa initially diverged and whether they have experienced secondary contact before the current interglacial period. Today, multiple reproductive barriers expressed at the Pyrenean hybrid zone are hypothesized to effectively balance dispersal, maintaining stable boundaries at multiple phenotypic clines as expected for tension zones (Butlin & Hewitt, 1985; Butlin et al., 1991). Using experimental crosses between parental individuals removed from the hybrid zone, several studies have shown that current reproductive barriers include: (i) premating behavioural isolation (Ritchie et al., 1989), (ii) postmating–prezygotic isolation (Bella et al., 1992) and (iii) postzygotic isolation (Virdee & Hewitt, 1992). Neither premating nor postzygotic barriers are stronger between populations closer to the hybrid zone centre (Ritchie et al., 1989; Virdee & Hewitt, 1994), rejecting expectations for reinforcement of reproductive isolation following secondary contact. Notably, in both hybrid zones, postzygotic isolation causes low fitness in reciprocal F_1 males (X0) through severe testis dysfunction, disrupted meiosis and full sterility, but not F_1 females (XX), conforming to Haldane's rule (Flanagan, 1997; Hewitt et al., 1987). Backcrosses of fertile F_1 females show some recovery of male sterility (Virdee & Hewitt, 1992, 1994). None of these reproductive barriers are noticeable in natural populations from the centre of the hybrid zones, suggesting that fitness recovery is possible through recombination and selection against incompatibilities. Nothing is known regarding patterns of gene flow across hybrid zones, besides limiting evidence from one allozymic marker (Butlin, 1998), two mitochondrial markers (e.g., Pereira et al., 2021) and from heterochromatin banding of the X chromosome (e.g., Serrano et al., 1996).

Although the *P. parallelus* hybrid zone was early recognized as "a window into the evolutionary process" (Harrison, 1993) and "a natural laboratory for evolutionary studies" (Hewitt, 1993), its large (14.72 Gb) and highly repetitive genome has prevented genetic studies using traditional Sanger and whole genome sequencing methods. Using RNA sequencing methods, we use the *P. parallelus* system to understand how quickly strong reproductive barriers evolve, and to understand their consequences for maintaining genetic boundaries between subspecies and populations. First, we identify evolutionarily independent units within *P. parallelus*, and infer their divergence time and phylogeographical history. Second, we test if pairs of lineages exhibiting hybrid male sterility have diverged in the presence of gene flow, and whether this is associated with repeatable patterns of genomic differentiation.

2 | MATERIALS AND METHODS

2.1 | Sampling and sequencing

To understand the phylogeographical history of *Pseudochorthippus parallelus*, we sampled 10 localities covering the known evolutionary lineages within this species (Figure 1a and Table S1). For the subspecies *P. p. erythropus*, we have sampled a population near its putative refugium in the Iberian Central System, a second in Portugal and a third neighbouring the Pyrenean hybrid zone. For the subspecies *P. p. parallelus*, we have sampled the lineage that putatively originated from a range expansion from a Balkan refugium (Lunt et al., 1998) in two populations within the central European range (Austria and Slovenia), plus two populations neighbouring the Pyrenean and Alpine hybrid zones. We have also sampled the *parallelus* that putatively originated from the Italic refugium, south of the Alpine hybrid zone. Additionally, we sampled populations near the putative centres of the Pyrenean and Alpine hybrid zones, following earlier cytogenetic studies (Flanagan et al., 1999; Zabal-Aguirre et al., 2010). In every locality we sampled five male individuals in close proximity. In some cases, two nearby sublocalities were sampled to capture a representative amount of diversity (see Table S1 for details; NCBI BioProjects PRJNA807476 and PRJNA801336). All specimens were sampled for this study, with the exception of the reference parental populations neighbouring the Pyrenean hybrid zone (PAR, ERY), which were published in a previous study (Nolen et al., 2020; NCBI BioProject PRJNA665162). Additionally, we used published data from five individual males of *Chorthippus biguttulus* sampled in Germany, used as an outgroup (Berdan et al., 2015; NCBI BioProject PRJNA284873).

In the field, we preserved whole body tissue in RNAlater (Qiagen) to sample the largest variety of transcripts possible. We excluded the head and upper digestive tract to avoid gut contamination and overrepresentation of eye pigments. In the laboratory, we homogenized the samples using ceramic beads (1.4/2.8 mm, Precellys) and the standard Tri-Reagent protocol (Sigma). We resuspended and purified RNA pellets with RNAeasy Mini columns (Qiagen), followed by a quantity and integrity check using an Agilent 2100 BioAnalyser. The Beijing Genomics Institute performed mRNA enrichment, library construction and paired-end Illumina HiSeq2500 sequencing. The three populations from the Pyrenees had a sequencing average of 59,391,201 paired reads (*SD*: 6,908,681) of 150 bp, while the remaining seven populations had a sequencing average of 49,410,055 (*SD*: 1,718,007) paired reads of 100 bp.

2.2 | Mapping and filtering

We used the BAM pipeline implemented in Paleomix (Schubert et al., 2014) for processing raw data. This process first removed adapters and trimmed low-quality bases (min. quality-offset for Phred scores 33) with ADAPTERREMOVAL (Schubert et al., 2016). Overlapping pairs were collapsed into one consensus read. All reads were then mapped
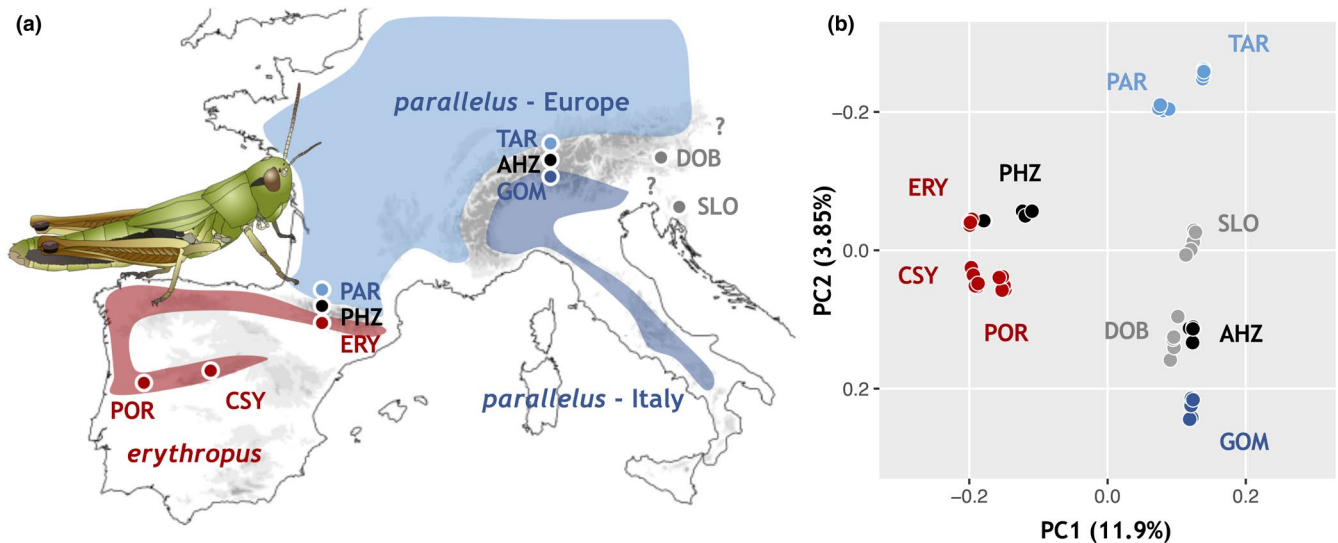
FIGURE 1 Divergence of *Pseudochorthippus parallelus*. (a) Sampling localities (dots) are coloured by their presumed evolutionary lineage according to subspecies and chromosomal race. Sampling localities in Eastern Central Europe (grey) and in the hybrid zones (black) cannot be attributed a priori to any lineage. (b) Principal component analysis based on 1,494,335 polymorphisms separates subspecies in PC1 and the chromosomal races of *P. p. parallelus* in PC2

with BWA-MEM, discarding poorly mapped reads under a quality threshold of 30 (Li & Durbin, 2009) against the reference transcriptome previously assembled and annotated by Nolen et al. (2020). These transcripts are organized in four partitions consisting of: (i) 16,969 single-copy genes, including 12,735 genes with identified open reading frames (ORFs) and 4,235 genes without; (ii) 4,263 multicopy genes; (iii) 18,623 genes found only in some individuals; and (iv) the complete mitochondrial genome. We visualized the number of nucleotides retained and coverage in partition 1 and 4 to assess the differences in coverage across localities (Figure S1).

As phylogenetic inference requires genotype calling, we produced haplotypes for the ORFs of the 12,735 single-copy nuclear genes and for the 13 mitochondrial genes, calling the most frequent base at each position with a minimum coverage threshold of 10×, using ANGSD version 0.921 (Korneliussen et al., 2014). As most of the population genetics inference can handle uncertainty of genotypes, which is particularly important with RNAseq data where coverage varies with gene expression, we estimated genotype likelihoods using ANGSD. For this data set, we used the 12,735 single-copy nuclear genes with identified ORFs, excluding the first and second codon positions that often correspond to nonsynonymous substitutions and hence are more affected by selection. We excluded reads with mapping quality <15 after adjustment, base read quality <20 or containing multiple hits. Additionally, we only considered sites present in a minimum of 80% of individuals, and with a coverage depth greater than twice the total number of individuals (see https://github.com/lindington/ChorthPar for the detailed commands).

2.3 | Population structure and admixture

To assess population structure and identify ongoing hybridization, we used the population genetics data set. First, we performed a principal component analysis (PCA) with NGSPOPGEN (Fumagalli et al., 2014) to test if genetic variation reflects the spatial distribution of the samples. We considered only variable sites with an SNP p-value $<1.0 \times 10^{-2}$ (i.e., in 1,494,335 SNPs), which has been shown to accurately reflect the site frequency spectrum based on all sites (Nolen et al., 2020). We expect most of the variance (PC1) to reflect subspecies and subsequent principal components to reflect known evolutionary lineages within subspecies. Second, we estimated admixture proportions in each individual, using the clustering algorithm implemented in NGSADMIX (Skotte et al., 2013), which maximizes Hardy–Weinberg and linkage equilibria within K ancestral clusters. We considered K from 2 to 11, the number of sampling localities (10) plus the outgroup, with 50 replicates, selecting the replicate with the highest likelihood for each. Because of the inclusion of the outgroup, this analysis is based on 708,874 SNPs. Analysis using no outgroup provided the same cluster assignments (results not shown). Under a mutation-drift equilibrium, we expect each subspecies or sampling locality to form a cluster, with possible admixture near the centre of the hybrid zones.

2.4 | Mitochondrial molecular clock

To infer the timing of diversification of the species we estimated a mitochondrial time tree. For this, we considered the 13 protein-coding genes to ensure site homology and avoid assembly and mapping errors in noncoding parts of the mitogenome. First, we aligned the 55 complete mitogenomes, annotated them using MITOS (Bernt et al., 2013) and extracted the alignments for the 13 protein-coding genes using a custom script (https://github.com/lindington/ChorthPar/). Second, we verified the absence of internal stop codons along the sequence with MEGA version 10.1.6 (Tamura et al.,

2007), and concatenated the genes. Third, we imported the concatenated alignment into IQ-TREE version 1.6.3 (Nguyen et al., 2015), estimated best-fit models of evolution for each gene using the BIC (Bayesian information criterion) score as implemented in MODELFINDER (Kalyaanamoorthy et al., 2017), and assessed branch support using 1,000 replicates of ultrafast bootstrapping (Hoang et al., 2018). The resulting maximum-likelihood (ML) tree carries the uncertainty of the estimated topology (Figure S2). Finally, we inferred divergence times using BEAST version 1.10.4 (Suchard et al., 2018). We used the uncorrelated relaxed clock model (Drummond et al., 2006), with a normally distributed prior for the substitution rate with mean 0.0115 and SD 0.001 substitutions per million years (Brower, 1994), which is appropriate given the remarkably conserved mitochondrial rates in insects (e.g., 0.0115 in butterflies and 0.0133 in beetles; Brower, 1994; Papadopoulou et al., 2010, respectively). The tree topology was fixed to the previously inferred ML topology, and we used a birth–death prior for speciation (Gernhard, 2008). BEAST runs were initialized with a chronogram based on the ML tree and the divergence time between *P. p. erythropus* and *P. p. parallelus* was set to a minimum age of 15 thousand years ago (ka) (end of the last glacial maximum; Ivy-Ochs et al., 2008) and a maximum age of 33.9 million years ago (the oldest Acrididae fossil; Song et al., 2018), using the R package *ape* (Paradis & Schliep, 2019). To facilitate convergence, tree topology, clock model and substitution model (GTR) were linked across genes. Three independent Markov chain Monte Carlo (MCMC) chains were run for 100 million generations, after a burn-in of 10 million, and sampling every 10,000 generations. We checked for convergence a posteriori using TRACER version 1.7.1 (Rambaut et al., 2018), and that all ESS values were above 200. We merged the independent chains using LOGCOMBINER and estimated divergence times using TREEANNOTATOR after discarding the initial 10 million generations of burn-in.

2.5 | Nuclear species tree

To assess the evolutionary relationships between sampling populations, we inferred a nuclear species tree under the multispecies coalescent model, which accommodates incomplete lineage sorting (ILS) expected for rapid radiations (Degnan & Rosenberg, 2009). First, we extracted the coding regions of the 12,735 single-copy nuclear genes for which ORFs were identified to avoid biases caused by assembly errors or under-expressed areas of the transcriptome, such as untranslated regions (UTRs), which could increase the uncertainty of the estimated gene trees. Second, we retained all genes that had more than 300 called positions, and that were present in a minimum of three out of the five individuals per population. Third, we inferred an ML tree for every individual nuclear gene using IQ-TREE version 1.6.3 (Nguyen et al., 2015) using BIC-selected models, 1000 replicates of ultrafast bootstrapping (UFBoot), and SH-like approximate likelihood ratio tests (SH-aLRT; Guindon et al., 2010; Hoang et al., 2018). To account for the uncertainty in gene tree estimation, we collapsed branches with <50% UFBoot support. Fourth, we assessed

the information content of each nuclear gene tree and compared it to the mitochondrial tree (Strimmer & Haeseler, 1997), performing a likelihood quartet mapping test in IQ-TREE. Finally, we estimated the species tree that maximizes the topology agreement between independent nuclear gene trees (Mirarab & Warnow, 2015), using ASTRAL version 5.6.1 (Mirarab et al., 2014). From this analysis, we output the main species tree topology, posterior probabilities for this main topology, and branch lengths in coalescent units (T/N_e; Degnan & Rosenberg, 2009). We used this approach to estimate (i) an "individual species tree" where each individual is a terminal branch, and (ii) a "population species tree" where individuals sampled in the 10 sampling localities are grouped together (as in Table S1). We expect the subspecies to form two reciprocally monophyletic groups with hybrid individuals or populations having an intermediate position in the species tree.

2.6 | Gene flow between populations

To test for the presence and magnitude of gene flow between all sampled populations, we used Patterson's *D*-statistics (Durand et al., 2011). This test weights the fraction of biallelic sites that have a different topology from the previously estimated species tree. Using *C. biguttulus* as the outgroup carrying the ancestral A allele, we measured the proportion of ABBA and BABA sites for all possible combinations of three *P. parallelus* taxa that conformed to our estimated species tree (i.e., in 120 comparisons). We used Abbababa2 as implemented in ANGSD, which extends this analysis to comparisons among populations (Soraggi et al., 2018). We restricted the analysis to sites with an SNP *p*-value $<1.0 \times 10^{-6}$ and estimated significance using a *p*-value calculated from 10 windows of ~240,000 relevant sites. A similar proportion of ABBA and BABA ($D = 0$) sites is expected under the null hypothesis of ILS driving discordance, while significantly different proportions ($D \neq 0$ with *p*-value $< .05$) must be explained by gene flow between two populations. We visualized Patterson's *D*-statistics using a matrix of all possible pairwise comparisons (i.e., excluding sister taxa), using the highest reached *D*-value for each comparison. If hybrid male sterility does not confer a genome-wide barrier to introgression, or if past introgression occurred before the emergence of strong reproductive isolation, we expect to find high *D*-statistics between populations located on either side of the Pyrenean and Alpine hybrid zones.

2.7 | The demographic history of hybrid zones

To quantify the relative amount of divergence and gene flow across the two hybrid zones, we estimated the demographic history of divergence of pairs of parental taxa at each zone separately (ERY vs. PAR for the Pyrenees, and TAR vs. GOM for the Alps). We considered four nested demographic models: (i) divergence without gene flow ("No Migration," with three parameters: time since population split T_1, and effective population size N_e

for each population); (ii) divergence with continuous gene flow ("Symmetric Migration," with a fourth migration rate parameter m); (iii) gene flow after secondary contact ("Secondary Contact," with the fifth parameter time since secondary contact T_2, after which migration starts); and (iv) divergence with asymmetric gene flow after secondary contact ("Secondary Contact with Asymmetric Migration," with the sixth m_2 parameter). First, we used ANGSD to build two-dimensional site frequency spectra (2D-SFSs) for each of the 16,969 single-copy nuclear genes and summed them into a single complete 2D-SFS per population pair. Second, the complete 2D-SFS was fit to all four demographic models using the diffusion approximation methods implemented in δaδi version 2.0.5 (Gutenkunst et al., 2009), as described in Nolen et al. (2020; see https://github.com/zjnolen/chorthippus_radiation for commands), with four technical replicates to guarantee convergence of the estimated parameter values. Finally, we compared nested models using a likelihood ratio test (LRT), and estimated parameter uncertainties with the Godambe Information Matrix (Coffman et al., 2016; Godambe, 1960), which uses 100 nonparametric bootstrap SFSs to account with physical linkage of SNPs within the same transcript. This procedure selects the simplest model that captures most of the demographic signal contained in the 2D-SFS, and thus we chose a model that is highly supported in both hybrid zones in order to compare demographic parameters. The demographic parameters T and $2Nm$ were estimated with reference to the constant mutation rate μ, as μ is probably the same for such closely related populations.

2.8 | Heterogeneity of gene flow

To estimate the relative effective population size for each sampling locality, we calculated per-gene Watterson's θ (Watterson, 1975) and π (Nei & Li, 1979). We also estimated deviation from a neutral model of constant population size by calculating per-gene Tajima's D (T_D; Tajima, 1989). For each summary statistic, we first built the one-dimensional SFS for each population and then calculated θ, π and T_D for each site in ANGSD. We used a custom script to average values across linked sites within each gene and plotted their distributions for the genes sampled across all populations (https://github.com/lindington/ChorthPar). We expect to find T_D closer to zero in populations sampled near the putative glacial refugia, and negative values in populations sampled near the edge of post-glacial range expansions.

To test if the same genes show highest differentiation across the two hybrid zones, we estimated pairwise F_{ST} (Reynolds et al., 1983) between pairs of parental populations interacting at each hybrid zone (ERY vs. PAR in the Pyrenees, and TAR vs. GOM in the Alps). We used the 2D-SFSs from demographic analyses to calculate a per-site and per-gene F_{ST} as implemented for other summary statistics. Using Fisher's exact test (Fisher, 1922) as implemented in the R package GeneOverlap (Shen, 2021), we tested if there is significant overlap between genes with the highest 5% F_{ST} in the two hybrid zones, as

expected in conformity with repeatable patterns of genetic differentiation. Because high F_{ST} can be caused either by gene-specific selection against gene flow or evolutionary constraints (Nachman & Payseur, 2012), we estimated d_{XY} (Nei & Li, 1979). We used ANGSD and a script adapted from Peñalba (https://github.com/mfumagalli/ngsPopGen/blob/master/scripts/calcDxy.R) to estimate per-site and per-gene d_{XY} as described above. We estimated the direction and significance of the correlation between F_{ST} and d_{XY} estimates using a linear model. If high F_{ST} is caused by selection counteracting gene flow, we expect a positive correlation, while if high F_{ST} is caused by strong drift caused by shared genomic constraints, we expect a negative correlation.

3 | RESULTS

3.1 | Mapping and filtering

Overall, trimming and mapping efficiency was equivalent across populations (Table S2). The percentage of retained nucleotides after filtering ranged from 79% to 89%, and mapping efficiency of reads ranged from 84% to 90% (Figure S1). The mitochondrial genome had a coverage between 16,000× and 52,000×, reflecting its expected high transcription levels. The single-copy nuclear genes with an identified ORF had a coverage between 46× and 125× (Figure S1), largely reflecting sequencing effort, which was larger in the Pyrenean populations (ERY, PHZ and PAR).

3.2 | Population structure

A relatively large fraction of the genetic variance (11.9%) is explained by principal component (PC) 1, which separates individuals of the two subspecies, reflecting a west–east gradient (Figure 1b). PC2 explains 3.85% of the variance and distinguishes individuals of the two evolutionary lineages known within the subspecies *Pseudochorthippus parallelus parallelus*, reflecting a north–south gradient. PC3 and PC4 explain 3% and 2.8% of the variance, respectively, and distinguish the Austrian samples (DOB) from all others (Figure S3).

Results from our admixture analysis show a continuously increasing likelihood for models with an increasing number of K ancestral clusters (Table S3). The first split within *P. parallelus* distinguishes the two subspecies, with some individuals from the Pyrenean hybrid zone showing similar admixture proportions (Figure 2b). Next, the European and Italian lineages of *P. p. parallelus* separate, also with similar admixture proportions found across individuals from the Alpine hybrid zone and the two locations closer to the Balkans (DOB and SLO). The Austrian population (DOB) becomes distinct at $K = 5$ and does not show admixture with any of the neighbouring localities (Figure 2b). At $K = 11$ each sampling locality forms its own cluster (Figure S4), with admixture found only in two individuals collected closer to the reference population of *P. p. erythropus* of the Pyrenees (Table S1).
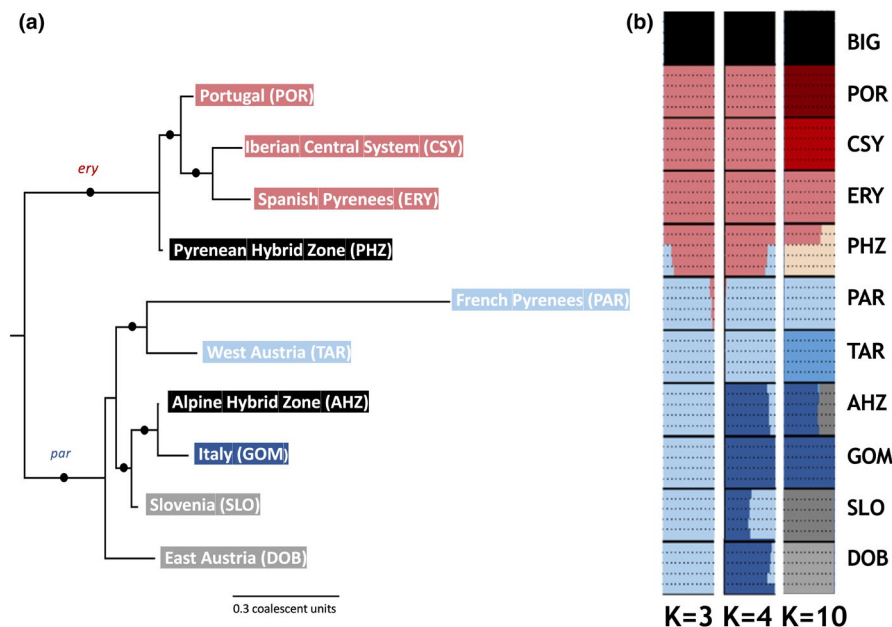
(a)

(b)

3.3 | Mitochondrial molecular clock

The ML mitochondrial tree (Figure S2) shows a well-supported topology (bootstrap [BP] values >95), where the two subspecies and most of the populations are not reciprocally monophyletic. The mitochondrial lineages form six major clades (A–F), most of them containing lineages found in a single subspecies. The exception are clades A and F, which contain internal nodes that separate *P. p. parallelus* and *P. p. erythropus*. We used those internal nodes to estimate the mean divergence time between subspecies.

The time to the most recent common ancestor (TMRCA) of all *P. parallelus* is estimated to be around 390 ka (95% highest posterior density: 432–322; Figure 3). The diversification of the six major clades ranges from 218 to 388 ka (Table S4). The TMRCA between subspecies in clades A and F occurred simultaneously, around 100 ka (128–66).

3.4 | Nuclear species tree

After filtering, we obtained 5,929 genes that were used for estimation of species trees. The likelihood mapping analysis shows that most gene trees have enough power to resolve 60%–80% of the quartets, reflecting high information content of nuclear gene trees (Figure S5). Individual gene trees show a wide range of sorting between alleles from each subspecies, from high gene tree discordance similarly to the mitochondrial genome, to two reciprocally monophyletic clades (Figure S6).

The individual species tree (Figure S7) shows that *P. p. erythropus* and *P. p. parallelus* are reciprocally monophyletic. Most populations form monophyletic clades (posterior probability, PP = 1) with only three exceptions. Individuals from the two sublocalities of the Pyrenean hybrid zone, sampled only 700 m apart, cluster separately: la Troya individuals form a sister clade to the

reference *erythropus* of the Pyrenees (ERY: sublocalities Biescas and Escarrilla, sampled 12 km apart), and Corral de Mulas individuals group as another paraphyletic grade at the base of the *P. p. erythropus* clade. Individuals from the two sublocalities of the *parallelus* from the Pyrenees (PAR: Gabas and Arudy, sampled 25 km apart) form a paraphyletic grade to a clade containing all individuals from West Austria (TAR). Finally, individuals from the Alpine hybrid zone (AHZ) also form a paraphyletic grade to a clade containing all Italian individuals (GOM).

The relationships between populations are well established in the "population species tree," where all branches have a support with PP >0.95 (Figure 2a). In agreement with the "individual species tree," populations of *P. p. erythropus* and *P. p. parallelus* are reciprocally monophyletic (PP >0.95). In the *erythropus* clade, the Pyrenean hybrid zone (PHZ) branches off first, followed by the Portuguese population (POR), and the reference *erythropus* of the Pyrenees (ERY) being sister to the population located in the putative glacial refugium at the Iberian Central System (CSY). The *parallelus* clade shows an early split of the East Austrian population (DOB), followed by a split between a clade containing the north European populations (PAR and TAR) from another clade comprising the southern European populations (SLO, GOM), including the Alpine hybrid zone (AHZ).

3.5 | Gene flow between populations

Out of the 360 possible comparisons, 120 conform to our nuclear species tree (Figure 2a). From these, 114 have *D*-statistics that are significantly different from zero ($p < .01574$; Table S5), consistent with gene flow between 34 population pairs (Figure 4). The remaining six population pairs show no significant deviations from the null expectation of no gene flow, and three population pairs could not be tested because they are sister taxa. All populations experience gene flow with at least one nonsister taxon. Notably, populations closer
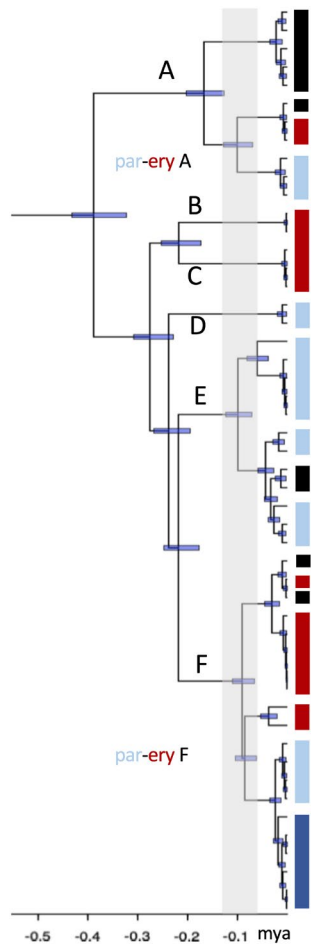
FIGURE 3 Time-calibrated tree based on 13 mitochondrial genes. Evolutionary lineages are coloured in terminal branches following Figure 1. Branch lengths are scaled in millions of years, and boxes on nodes represent 95% confidence intervals. The most recent common ancestor dates to 0.338 Ma, subsequently splitting into six major clades (A–F). Subspecies do not form monophyletic clades, with the exception of subclades A and F, which split around 100 ka (nodes marked as "par-ery"; Table S4 and Figure S2)

FIGURE 4 Extensive interpopulation gene flow throughout *Pseudochorthippus parallelus*. The heat map depicts the highest absolute *D*-statistic per population pair, estimated from 120 possible comparisons. All shaded comparisons were significant (*p* < .05); white comparisons were not significant; grey comparisons cannot be tested (Table S5)

for an increased number of parameters using the adjusted LRT, we find that the simplest model that can explain the observed SFS is the "Symmetric Migration" model for the Pyrenean hybrid zone, and in the "Secondary Contact" model for the Alpine hybrid zone (Table S6).

To allow comparisons across hybrid zones, we thus chose the simpler "Symmetric Migration" model for parameter estimation. Estimated N_e values of parental populations are similar in the Alpine hybrid zone, but they show a two-fold difference with nonoverlapping standard deviations in the Pyrenean hybrid zone (*parallelus* > *erythropus*). The parameter estimation converged on older divergence time *T* (Pyrenees: 0.0021; Alps: 0.0016; ~1.3 times older) and lower 2*Nm* (Pyrenees: 0.143 and 0.288; Alps: 0.294 and 0.333; mean ~0.7 times lower) for the Pyrenean hybrid zone relative to the Alpine hybrid zone, but with overlapping standard deviations (Table S7).

3.7 | Heterogeneity of gene flow

Distributions of per-gene Watterson's θ and π (Figure S8) were centred close to zero with populations differing in the length of the tail of the distribution and in their mean. Mean π varied between 0.0026 (CSY) and 0.0033 (PAR), with higher values found in the Pyrenean and Alpine hybrid zones, in the admixed population of Slovenia, and in the population of *parallelus* from the Pyrenees (PAR). A similar trend was observed in means of per-gene Watterson's θ, varying between 6.594 (CSY) and 9.330 (PAR), with the population of Portugal also showing high diversity.

The distributions of per-gene Tajima's *D* were generally centred around negative values in all populations (Figure 5), consistent with a general demographic expansion. Populations located in proximity

to the Pyrenean hybrid zone show the highest values of *D*-statistics across comparisons; that is, the reference *parallelus* population in France (PAR) consistently shows high gene flow with all populations of *erythropus* from Iberia, and conversely the Pyrenean hybrid population (PHZ) consistently shows high gene flow with all populations of *parallelus*. The Slovenian population (SLO) also shows high values of *D*-statistics with the Italian population (GOM and AHZ), also consistent with gene flow.

3.6 | The demographic history of hybrid zones

In our demographic models, all technical replicates converged to similar likelihoods and parameter estimations. The model with the highest likelihood is the most parameter-rich (i.e., the "SC with Asymmetric Migration" model). Yet, when penalizing the likelihoods
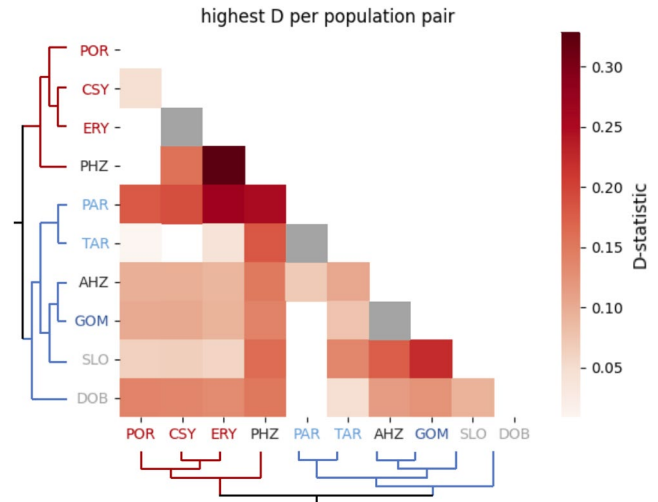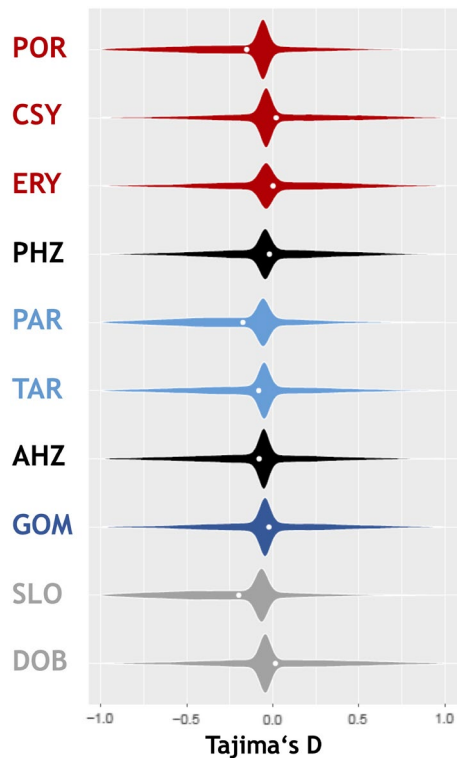
FIGURE 5 Deviations from demographic neutrality. Violin plots represent the distribution of Tajima's *D* calculated for 16,969 genes sampled across the 10 populations of *Pseudochorthippus parallelus*, and the white dot represents the gene-mean across the transcriptome

to putative refugia (CSY for *erythropus*, and GOM for the Italian *parallelus*) have means closest to zero, suggesting a smaller deviation from neutrality and thus relatively more demographic stability. Notably, in the eastern Austrian population (DOB) and in the southern Pyrenean population (PAR) we find means close to zero, also conforming to expectations of relative demographic stability. We found the most negative Tajima's *D* in populations further away from the known refugia (POR for *erythropus*, and PAR for the northern European *parallelus*), consistent with a stronger range expansion. Notably, the Slovenian population SLO has a similarly negative Tajima's *D*, also conforming to expectations of demographic range expansion.

The distributions of per-gene F_{ST} across the two hybrid zones are unimodal with a positive skew and medians of 0.235 and 0.357 for the Alpine and Pyrenean hybrid zones, respectively. Genes in the highest 5% per-gene F_{ST} have values above 0.63 for the lineages of *parallelus* hybridizing in the Alps, and above 0.74 for the subspecies hybridizing in the Pyrenees. Out of these 575 genes, 117 overlap, which is not expected to occur by chance ($p = 1.1 \times 10^{-41}$). Per-gene d_{XY} distributions are also unimodal and with positive skews in both hybrid zones (Figure S9). We found a significant negative correlation (slope = −0.0150551; $p < 2 \times 10^{-16}$) between d_{XY} and F_{ST} (Figure 6b) in both hybrid zones, consistent with shared genomic constraints across populations.

4 | DISCUSSION

Late stages of species formation are characterized by the accumulation of multiple reproductive barriers, that together result in full or nearly complete reproductive isolation. Understanding how quickly these barriers evolve and how effectively they can prevent gene flow between emergent species requires studying taxa exhibiting such late barriers that hybridize in nature. We provide some answers to these questions using lineages of the grasshopper species *Pseudochorthippus parallelus*, which express multiple pre- and postzygotic barriers, including hybrid male sterility in experimental hybrid laboratorial crosses (Flanagan, 1997; Hewitt et al., 1987), but have been interacting in two hybrid zones for thousands of generations (Butlin, 1998; Hewitt, 1993).

4.1 | The phylogeographical history of *P. parallelus*

P. parallelus has been fundamental for our current understanding of biogeographical patterns in Europe (Hewitt, 2000) and was early recognized as an important window into species formation (Barton & Hewitt, 1985; Futuyma et al., 1995). Early studies based on small mitochondrial DNA fragments presented a relatively simple scenario of divergence in three southern glacial refugia (Iberia, Italy, Balkans; Cooper et al., 1995) and the evolution of multiple reproductive barriers, including hybrid male sterility (Hewitt et al., 1987; Shuker et al., 2005). However, understanding how reproductive barriers evolved requires estimating the time of divergence between these lineages and their phylogeographical history.

Our estimated mitochondrial time tree based on the complete mitochondrial genome places the TMCRA of all *P. parallelus* in the mid-Pleistocene, around 389,000 years ago (95% highest posterior density [HPD]: 432,200–322,600; Figure 3 and Table S4). Similarly to what we found in thousands of independent nuclear gene trees (Figure S6), the mitochondrial tree shows extensive allele sharing between subspecies (Figures 3 and S2). Such patterns of allele sharing are often observed in other insects characterized by large effective population sizes and interspecific gene flow (Ebdon et al., 2021; Pollard et al., 2006), including in grasshopper species of the related genus *Chorthippus* (Nolen et al., 2020), suggesting that both ILS and gene flow probably underlie such patterns. Two out of the six mitochondrial clades have sublineages that are fixed among subspecies (nodes within clades A and F, Figure 3), allowing us to estimate a minimum time of divergence between the two subspecies *P. p. parallelus* and *P. p. erythropus*. In both clades, divergence is estimated to have occurred around 100,000 years ago (127,900–65,900), placing divergence time at the beginning of the last glacial cycle in Europe (Ganopolski & Brovkin, 2017).

Using information from nuclear genes we were able to establish a well-supported phylogeographical scenario for the diversification of *P. parallelus* in Europe. As expected, the oldest split occurred between the two subspecies (Figures 2a and S7), reflecting the oldest vicariant event between the Iberian Peninsula, where *erythropus*
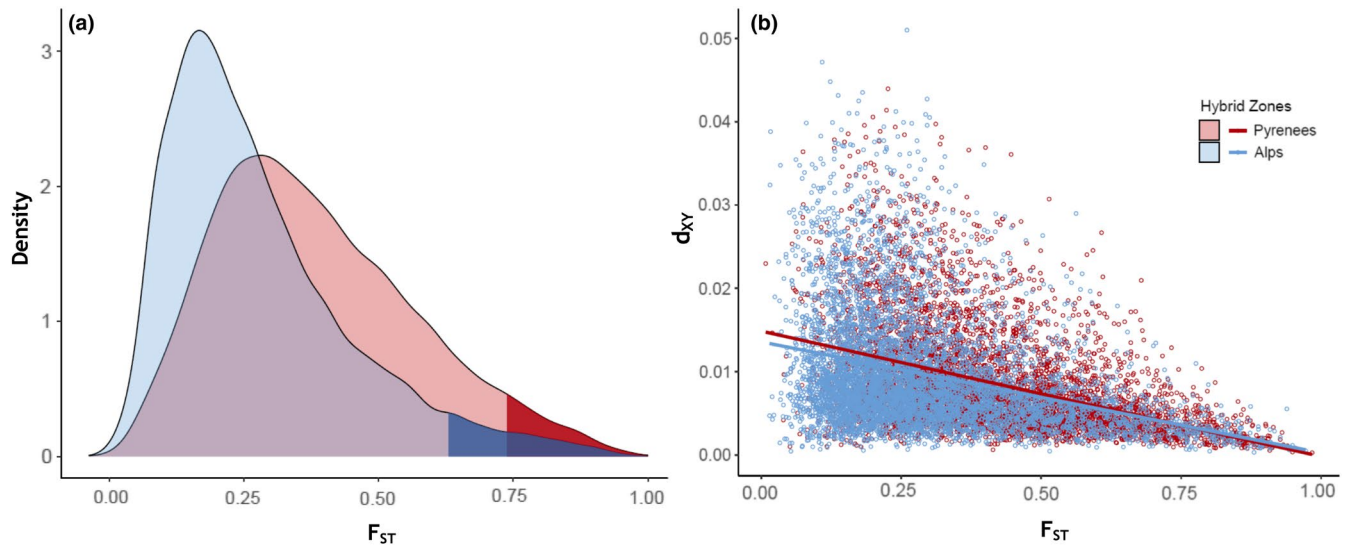
FIGURE 6 Repeatable patterns of genomic differentiation across two hybrid zones manifesting hybrid male sterility. (a) Density of per-gene estimates of F_{ST} in 11,503 genes sampled both in the Pyrenean (red) and in the Alpine (blue) hybrid zone, showing a significant overlap of 117 genes within the 95th percentile ($p = 1.1 \times 10^{-41}$). (b) In both hybrid zones, per-gene differentiation (F_{ST}) is negatively correlated with per-gene divergence (d_{XY}; $p < 2.2 \times 10^{-16}$), consistent with a strong contribution of linked selection in the repeatable patterns of genomic differentiation

diverged and remains isolated, and the ancestor of *parallelus*. The population near the centre of the Pyrenean hybrid zone is at the base of the *erythropus* clade, probably due to introgression from *parallelus* that is not accounted for in the multispecies coalescent, as clarified in the individual patterns of admixture (Figure 2b). Within the pure *erythropus*, we find evidence for an early split between a Portuguese (POR) and a Spanish lineages, followed by the colonization of the southern slope of the Pyrenees (ERY) from the Spanish side of the Iberian Central System (CSY). Patterns of genetic diversity (Tajima's *D*; Figure 5) suggest demographic stability at both Spanish localities, but with a stronger range expansion on the Portuguese side of the Iberian Central System. These observations are consistent with two subrefugia within Iberia, a recurrent phylogeographical pattern across Iberian plant and animal species that has been popularized as "refugia within refugium" (Feliner, 2011; Gómez & Lunt, 2007). Earlier cytogenetic work in *erythropus* (Bella et al., 1990) has shown the existence of two variants of the X chromosome that differ in the location of the active nucleolar organizing regions (NORs). Because NORs are associated with rDNA activity during meiosis, this finding suggests functional divergence of the sexual chromosomes of the Portuguese and Spanish *erythropus*. Future experimental crosses or study of a cryptic hybrid zone along the Iberian Central System can test whether such divergence has resulted in some degree of reproductive isolation within this subspecies.

Within the *parallelus* clade, we do not find evidence for an earlier split between the Italian and the Balkan lineages, as suggested by previous studies (Cooper et al., 1995), but rather for the divergence of the Austrian lineage located in the East of the Alps (DOB). This lineage is distinct from all other known lineages, including from the Balkans lineage detected in Slovenia (SLO). Notably, this population form a monophyletic clade that diverged around 100,000 years ago

(95% HPD: 123,400–71,100) from the remaining *parallelus* (Table S4 and Figure 3; split of DOB within clade A), does not hybridize with nearby populations (Figures 2B and S4), and has a Tajima's *D* consistent with demographic stability ($T_D = -0.217$; Figure 5). These observations are consistent with this population representing an old refugium for *parallelus*, suggesting that some relictual populations have survived the last glacial period in a microrefugium within the Alps, despite this large mountain system being largely glaciated until 15,000 years ago (Ivy-Ochs et al., 2008). Small isolated refugia have been demonstrated for alpine plants (Stehlik et al., 2002), beetles (Lohse et al., 2011) and in jumping bristletails (Wachter et al., 2012). The existence of species of grasshoppers micro-endemic to isolated regions of the Alps, such as *Podismopsis keisti* (Nadig, 1989) and *Podismopsis styriaca* (Koschuh, 2008), suggests that such Alpine refugia might have played an important role for current biogeographical patterns in Europe. The next split within *parallelus* refers to the vicariant event between the broadly distributed central European lineage and the Italian lineage. Previous studies have shown that these lineages diverged in one NOR at the distal end of the X chromosome (Flanagan et al., 1999) and give rise to sterile hybrid males in laboratory crosses (Flanagan, 1997). This suggests that genetic incompatibilities leading to hybrid male sterility can evolve fairly rapidly in this system.

In addition to relatively short divergence times, the demographic history of *P. parallelus* deviates strongly from neutral expectations (Figure 5). Notably, our estimates of Tajima's *D* are negative in populations on the northern slopes of mountain ranges known to have harboured important glaciers during the Pleistocene, such as the Iberian Central System (POR, $T_D = -0.169$), the Pyrenees (PAR, $T_D = -0.183$), the Alps (TAR, $T_D = -0.088$), and Slovenia (SLO, $T_D = -0.217$), consistent with demographic range expansions onto

northern slopes after the ice sheets retreated. This molecular signature of demographic expansion is strongest in the European lineage of *parallelus* in the French Pyrenees (PAR), which is genetically similar to the Austrian population (TAR) collected ~990 km away (Figure 1b) and shows the longest coalescent time (T/N_e) in the species tree (Figure 2a). The effect of strong genetic drift before secondary contact is further reflected in the relatively high F_{ST} values observed between taxa that established secondary contact, both in the Pyrenean (global F_{ST} =0.395) and in the Alpine (global F_{ST} =0.286) hybrid zones.

Together, this phylogeographical scenario shows that hybrid male sterility has evolved at least between three different lineages of *P. parallelus* that diverged relatively recently, within the last 389,000 years, corresponding to the same number of generations in this species. The evolution of hybrid male sterility is thus significantly faster relative to what has been estimated in well-studied systems, such as Drosophilids (that diverged more than 300,000 years or more than 2.4 million generations ago; Kliman et al., 2000) or the house mouse (that diverged 300–500 million years, or 200–333 million generations ago; Phifer-Rixey et al., 2020). Strong periods of genetic drift, not only caused by the allopatric divergence during the glacial periods, but also due to a strong range expansion during the current interglacial period, probably facilitated the fixation of incompatibilities that cause hybrid male sterility, among other reproductive barriers maintaining these hybrid zones.

4.2 | Gene flow between *P. parallelus* subspecies and populations

Although the reference populations sampled here in the Pyrenean hybrid zone are known to produce sterile F_1 males (Flanagan, 1997; Hewitt et al., 1987), backcrossing through fertile F_1 females leads to males with some, but largely reduced, fertility (Virdee & Hewitt, 1992). Strong (but not increased; Ritchie et al., 1992) hybrid male sterility is observed even between populations that are 4–6 km apart (Virdee & Hewitt, 1994), suggesting that it contributes as a strong barrier to gene flow in natural populations. Here, we test if long-term recombination in the hybrid zones has allowed for genetic introgression despite the multiple reproductive barriers observed in this system.

Our analyses show that the samples collected near the putative centres of the two hybrid zones are indeed admixed (Figures 1b and 2b), consistent with ongoing backcrossing in natural populations. The admixture proportions were similar across individuals near the centres of both hybrid zones, suggesting that hybrid populations are currently at a migration–drift equilibrium. Future sampling in transects perpendicular to the hybrid zones are required to clarify contemporary rates of hybridization and the geographical centres of the hybrid zones.

Demographic models of divergence between pairs of parental populations of both hybrid zones significantly rejected models of divergence without gene flow in favour of a model with symmetric gene flow ($p = 0$). Biologically more realistic models (e.g., secondary contact with symmetric or asymmetric migration) had higher likelihoods but were not significantly better, reflecting a limited power to estimate extra parameters (Table S6). Consistent with our estimated species tree (Figure 2a) and their levels of genetic differentiation (Table S8), we estimate that the lineages interacting in the Pyrenean hybrid zone are approximately more divergent (1.3 times) and experience less gene flow (0.7 times) than the lineages interacting in the Alpine hybrid zone. Given that the two hybrid zones are at the same altitude, probably have the same age (Palacios et al., 2017), and that the parental populations were sampled at a similar geographical distance (50 km), this suggests that barriers to gene flow are stronger between the subspecies *parallelus* and *erythropus* establishing secondary contact in the Pyrenees than between the two lineages of *parallelus* establishing contact in the Alps. Yet, caution is needed when interpreting these results, since the confidence intervals of the parameter estimates are overlapping (Table S7). Our estimates of the population migration rate $2Nm$ (Pyrenees: 0.143 and 0.288; Alps: 0.294 and 0.333) indicate that genetic drift is stronger than gene flow ($2Nm < 1$; Slatkin, 1985). Yet, these estimates are probably an underrepresentation of the true effective migration rates experienced at the centre of the hybrid zone because these parental populations are geographically isolated and estimates of $2Nm$ are averaged over the entire divergence time in such simplistic models (Hamilton et al., 2005).

Using the ABBA–BABA-test, we infer the amount of introgression across all pairs of populations. We observe that, except for six population pairs, the remaining 36 possible pairs show significant gene flow ($p < .01574$, Figure 4). Notably, populations close to the hybrid zones show the highest level of introgression, even though these populations exhibit complete hybrid male sterility (Virdee & Hewitt, 1994). For example, the pure *parallelus* population of the French Pyrenees (PAR) shows abundant introgression with all *erythropus* populations ($D > 0.18$), which generally decreases with geographical distance. Conversely, the hybrid population of the Pyrenees shows strong introgression with all *parallelus* populations, also largely decreasing with geographical distance. While such patterns of introgression could be expected after reinforcement (ancient hybridization followed by evolution of reproductive isolation; Butlin, 1987; Coyne & Orr, 2004; Pfennig & Pfennig, 2012; Servedio & Noor, 2003), previous analyses have found no evidence of increased premating isolation or selection against hybrids in populations closer to the hybrid zone centre (Ritchie et al., 1992). Due to the lack of evidence for reinforcement, the observed patterns of introgression are more likely to be the consequence of one or multiple episodes of secondary contact during interglacial periods.

Numerous studies have found patterns of repeatable genomic differentiation associated with the repeated evolution of several forms of reproductive isolation, for example ecological incompatibilities in stick insects (Riesch et al., 2017) and marine snails (Westram et al., 2021), and behavioural incompatibilities in crows

(Poelstra et al., 2014) and newts (Zieliński et al., 2019). While high values of F_{ST} can in fact reflect barriers to gene flow in the genome, because F_{ST} depends on heterozygosity within populations, high F_{ST} can also reflect low divergence at those specific loci. Although we find overlap between genes exhibiting high values of F_{ST} in the two hybrid zones, we also find a negative correlation between F_{ST} and d_{XY} in both hybrid zones ($p < 2 \times 10^{-16}$). This suggests that the repeatable patterns of genomic differentiation in the two hybrid zones may be unrelated to locus-specific barriers to gene flow, but may simply reflect genomic constraints, such as low mutation, recombination rates, or linked selection and/or background selection experience in the ancestral population (Nachman & Payseur, 2012).

Together, these results suggest that, while late stages of species formation are characterized by strong pre- and postzygotic isolation, the rates of effective recombination that are observed in natural hybrid zones are enough to permit introgression in some parts of the genome. The observation that the amount of introgression decreases with the geographical distance to the current hybrid zone suggests that introgression is at least partially explained by gene flow after the recent secondary contact. The observation of extensive rates of introgression in spite of strong reproductive barriers has been described in multiple hybridizing systems, such as in birds (Poelstra et al., 2014; Semenov et al., 2021), butterflies (Heliconius Genome Consortium, 2012) and mice (Teeter et al., 2007). Future studies of differential patterns of introgression across the genome may help in pinpointing the genes that resist to such a prevailing pattern of genome-wide introgression (Rafati et al., 2018; Turner & Harr, 2014), and therefore that are involved in barriers to gene flow (Barton & Hewitt, 1989; Harrison & Larson, 2014).

CONFLICT OF INTEREST

The authors have no conflict of interest to declare.

AUTHOR CONTRIBUTIONS

Ricardo J. Pereira conceived the project, cofounded by Ricardo J. Pereira and Tamí Mott. Ricardo J. Pereira, Oliver Hawlitschek and José L Bella performed the sampling and Ricardo J. Pereira produced the data. Ricardo J. Pereira, Linda Hagberg and Enrique Celemín analysed the data and interpreted the results. Ricardo J. Pereira, Linda Hagberg and Enrique Celemín wrote the first version of the manuscript, and all authors contributed to the final version.

OPEN RESEARCH BADGES

This article has earned an Open Data Badge for making publicly available the digitally-shareable data necessary to reproduce the reported results. The data is available at https://github.com/lindington/ChorthPar.

DATA AVAILABILITY STATEMENT

Raw reads sequenced for this study were deposited in the NCBI Sequence Read Archive (BioProject PRJNA807476, BioSample Acc. SAMN25987978-SAMN25988015; and BioProject PRJNA801336, BioSample Acc. SAMN25339080–SAMN25339081). Reads obtained from other studies are accessible in the NCBI Read Archive (BioProject PRJNA284873, BioSample Acc. SAMN03733888–SAMN03733892, Berdan et al., 2015; BioProject PRJNA665162, BioSample Acc. SAMN16264388–SAMN16264397, Nolen et al., 2020). The dryad archive (doi: https://doi.org/10.5061/dryad.qnk98sfj6) contains: per-gene estimates of F_{ST}, d_{XY}, pi, theta and Tajima's D; mitochondrial and nuclear alignments for the phylogenetic analyses, and infiles for the admixture and demographic analyses. Bioinformatic scripts are available in a public GitHub repository: https://github.com/lindington/ChorthPar.

ORCID

Linda Hagberg https://orcid.org/0000-0003-1441-6931
Oliver Hawlitschek https://orcid.org/0000-0001-8010-4157
Ricardo J. Pereira https://orcid.org/0000-0002-8076-4822

REFERENCES

Barton, N. H., & Hewitt, G. M. (1985). Analysis of hybrid zones. *Annual Review of Ecology and Systematics*, 16(1), 113–148. https://doi.org/10.1146/annurev.es.16.110185.000553

Barton, N. H., & Hewitt, G. M. (1989). Adaptation, speciation and hybrid zones. *Nature*, 341(6242), 497–503. https://doi.org/10.1038/341497a0

Bateson, W. (1909). *Heredity and variation in modern lights*. Darwin and Modern Science.

Bella, J. L., Butlin, R. K., Ferris, C., & Hewitt, G. M. (1992). Asymmetrical homogamy and unequal sex ratio from reciprocal mating-order crosses between *Chorthippus parallelus* subspecies. *Heredity*, 68(4), 345–352. https://doi.org/10.1038/hdy.1992.49

Bella, J. L., Hewitt, G. M., & Gosálvez, J. (1990). Meiotic imbalance in laboratory-produced hybrid males of *Chorthippus parallelus parallelus* and *Chorthippus parallelus erythropus*. *Genetics Research*, 56(1), 43–48. https://doi.org/10.1017/S001667230002886X

Berdan, E. L., Mazzoni, C. J., Waurick, I., Roehr, J. T., & Mayer, F. (2015). A population genomic scan in *Chorthippus* grasshoppers unveils previously unknown phenotypic divergence. *Molecular Ecology*, 24(15), 3918–3930. https://doi.org/10.1111/mec.13276

Bernt, M., Donath, A., Jühling, F., Externbrink, F., Florentz, C., Fritzsch, G., Pütz, J., Middendorf, M., & Stadler, P. F. (2013). MITOS:

Improved de novo metazoan mitochondrial genome annotation. *Molecular Phylogenetics and Evolution*, 69(2), 313–319. https://doi.org/10.1016/j.ympev.2012.08.023

Bracewell, R. R., Bentz, B. J., Sullivan, B. T., & Good, J. M. (2017). Rapid neo-sex chromosome evolution and incipient speciation in a major forest pest. *Nature Communications*, 8(1), 1593. https://doi.org/10.1038/s41467-017-01761-4

Brower, A. V. (1994). Rapid morphological radiation and convergence among races of the butterfly *Heliconius erato* inferred from patterns of mitochondrial DNA evolution. *Proceedings of the National Academy of Sciences*, 91(14), 6491–6495. https://doi.org/10.1073/pnas.91.14.6491

Butlin, R. K. (1987). Speciation by reinforcement. *Trends in Ecology & Evolution*, 2(1), 8–13. https://doi.org/10.1016/0169-5347(87)90193-5

Butlin, R. K. (1998). What do hybrid zones in general, and the *Chorthippus parallelus* zone in particular, tell us about speciation. In *Endless forms: Species and speciation* (pp. 367–378). Oxford University Press.

Butlin, R. K., & Hewitt, G. M. (1985). A hybrid zone between *Chorthippus parallelus parallelus* and *Chorthippus parallelus erythropus* (Orthoptera: Acrididae): Behavioural characters. *Biological Journal of the Linnean Society*, 26(3), 287–299. https://doi.org/10.1111/j.1095-8312.1985.tb01637.x

Butlin, R. K., Ritchie, M. G., & Hewitt, G. M. (1991). Comparisons among morphological characters and between localities in the *Chorthippus parallelus* hybrid zone (Orthoptera: Acrididae). *Philosophical Transactions of the Royal Society of London. Series B: Biological Sciences*, 334(1271), 297–308. https://doi.org/10.1098/rstb.1991.0119

Christin, P.-A., Weinreich, D. M., & Besnard, G. (2010). Causes and evolutionary significance of genetic convergence. *Trends in Genetics*, 26(9), 400–405. https://doi.org/10.1016/j.tig.2010.06.005

Coffman, A. J., Hsieh, P. H., Gravel, S., & Gutenkunst, R. N. (2016). Computationally efficient composite likelihood statistics for demographic inference. *Molecular Biology and Evolution*, 33(2), 591–593. https://doi.org/10.1093/molbev/msv255

Cooper, S. J. B., Ibrahim, K. M., & Hewitt, G. M. (1995). Postglacial expansion and genome subdivision in the European grasshopper *Chorthippus parallelus*. *Molecular Ecology*, 4(1), 49–60. https://doi.org/10.1111/j.1365-294X.1995.tb00191.x

Coughlan, J. M., & Matute, D. R. (2020). The importance of intrinsic postzygotic barriers throughout the speciation process. *Philosophical Transactions of the Royal Society B: Biological Sciences*, 375(1806), 20190533. https://doi.org/10.1098/rstb.2019.0533

Coyne, J. A. (2018). "Two rules of speciation" revisited. *Molecular Ecology*, 27(19), 3749–3752. https://doi.org/10.1111/mec.14790

Coyne, J. A., & Orr, H. A. (1989). Patterns of speciation in Drosophila. *Evolution*, 43(2), 362–381. https://doi.org/10.1111/j.1558-5646.1989.tb04233.x

Coyne, J. A., & Orr, H. A. (2004). *Speciation* (Vol. 37).

Defaut, B. (2012). Implications taxonomiques et nomenclaturales de publications récentes en phylogénie moléculaire: 1. Les Gomphocerinae de France (Orthoptera, Acrididae). *Matériaux Orthoptériques Et Entomocénotiques*, 17, 15–20.

Degnan, J. H., & Rosenberg, N. A. (2009). Gene tree discordance, phylogenetic inference and the multispecies coalescent. *Trends in Ecology & Evolution*, 24(6), 332–340. https://doi.org/10.1016/j.tree.2009.01.009

Dobzhansky, T. (1936). Studies on hybrid sterility. II. Localization of sterility factors in *Drosophila pseudoobscura* hybrids. *Genetics*, 21(2), 113.

Drummond, A. J., Ho, S. Y., Phillips, M. J., & Rambaut, A. (2006). Relaxed phylogenetics and dating with confidence. *PLoS Biology*, 4(5), e88. https://doi.org/10.1371/journal.pbio.0040088

Durand, E. Y., Patterson, N., Reich, D., & Slatkin, M. (2011). Testing for ancient admixture between closely related populations. *Molecular Biology and Evolution*, 28(8), 2239–2252. https://doi.org/10.1093/molbev/msr048

Ebdon, S., Laetsch, D. R., Dapporto, L., Hayward, A., Ritchie, M. G., Dincă, V., Vila, R., & Lohse, K. (2021). The Pleistocene species pump past its prime: Evidence from European butterfly sister species. *Molecular Ecology*, 30(14), 3575–3589. https://doi.org/10.1111/mec.15981

Feliner, G. N. (2011). Southern European glacial refugia: A tale of tales. *Taxon*, 60(2), 365–372. https://doi.org/10.1002/tax.602007

Fisher, R. A. (1922). On the interpretation of χ^2 from contingency tables, and the calculation of P. *Journal of the Royal Statistical Society*, 85(1), 87–94. https://doi.org/10.2307/2340521

Flanagan, M., Mason, P. L., Gosalvez, J., & Hewitt, G. M. (1999). Chromosomal differentiation through an Alpine hybrid zone in the grasshopper *Chorthippus parallelus*. *Journal of Evolutionary Biology*, 12(3), 577–585. https://doi.org/10.1046/j.1420-9101.1999.00049.x

Flanagan, N. S. (1997). *Incipient speciation in the meadow grasshopper*, Chorthippus parallelus *(Orthoptera: Acrididae)* (PhD thesis). University of East Anglia.

Fumagalli, M., Vieira, F. G., Linderoth, T., & Nielsen, R. (2014). ngsTools: Methods for population genetics analyses from next-generation sequencing data. *Bioinformatics*, 30(10), 1486–1487. https://doi.org/10.1093/bioinformatics/btu041

Futuyma, D. J., Shapiro, L. H., & Harrison, R. G. (1995). Hybrid zones and the evolutionary process. *Evolution*, 49(1), 222. https://doi.org/10.2307/2410309

Ganopolski, A., & Brovkin, V. (2017). Simulation of climate, ice sheets and CO_2 evolution during the last four glacial cycles with an Earth system model of intermediate complexity. *Climate of the Past*, 13(12), 1695–1716. https://doi.org/10.5194/cp-13-1695-2017

Gernhard, T. (2008). The conditioned reconstructed process. *Journal of Theoretical Biology*, 253(4), 769–778. https://doi.org/10.1016/j.jtbi.2008.04.005

Godambe, V. P. (1960). An optimum property of regular maximum likelihood estimation. *The Annals of Mathematical Statistics*, 31(4), 1208–1211. JSTOR. https://doi.org/10.1214/aoms/1177705693

Gómez, A., & Lunt, D. H. (2007). Refugia within Refugia: Patterns of phylogeographic concordance in the Iberian Peninsula. In S. Weiss, & N. Ferrand (Eds.), *Phylogeography of Southern European Refugia: Evolutionary perspectives on the origins and conservation of European biodiversity* (pp. 155–188). Springer Netherlands. https://doi.org/10.1007/1-4020-4904-8_5

Gosálvez, J., López-Fernández, C., Bella, L. J., Butlin, R. K., & Hewitt, G. M. (1988). A hybrid zone between *Chorthippus parallelus parallelus* and *Chorthippus parallelus erythropus* (Orthoptera: Acrididae): Chromosomal differentiation. *Genome*, 30(5), 656–663. https://doi.org/10.1139/g88-111

Guindon, S., Dufayard, J.-F., Lefort, V., Anisimova, M., Hordijk, W., & Gascuel, O. (2010). New algorithms and methods to estimate maximum-likelihood phylogenies: Assessing the performance of PhyML 3.0. *Systematic Biology*, 59(3), 307–321. https://doi.org/10.1093/sysbio/syq010

Gutenkunst, R. N., Hernandez, R. D., Williamson, S. H., & Bustamante, C. D. (2009). Inferring the joint demographic history of multiple populations from multidimensional SNP frequency data. *PLoS Genetics*, 5(10), e1000695. https://doi.org/10.1371/journal.pgen.1000695

Haldane, J. B. S. (1922). Sex ratio and unisexual sterility in hybrid animals. *Journal of Genetics*, 12(2), 101–109. https://doi.org/10.1007/BF02983075

Hamilton, G., Currat, M., Ray, N., Heckel, G., Beaumont, M., & Excoffier, L. (2005). Bayesian estimation of recent migration rates after a spatial expansion. *Genetics*, 170(1), 409–417. https://doi.org/10.1534/genetics.104.034199

Harrison, R. G. (1990). Hybrid zones: Windows on evolutionary process. *Oxford Surveys in Evolutionary Biology*, 7, 69–128.

Harrison, R. G. (1993). Hybrids and hybrid zones: Historical perspective. *Hybrid Zones and the Evolutionary Process*, 3–12.

Harrison, R. G., & Larson, E. L. (2014). Hybridization, introgression, and the nature of species boundaries. *Journal of Heredity*, 105(S1), 795–809. https://doi.org/10.1093/jhered/esu033

Heliconius Genome Consortium. (2012). Butterfly genome reveals promiscuous exchange of mimicry adaptations among species. *Nature*, 487(7405), 94–98. https://doi.org/10.1038/nature11041

Hewitt, G. M. (1993). After the ice: Parallelus meets erythropus in the Pyrenees. *Hybrid Zones and the Evolutionary Process* (pp. 140–164).

Hewitt, G. M. (2000). The genetic legacy of the Quaternary ice ages. *Nature*, 405(6789), 907–913. https://doi.org/10.1038/35016000

Hewitt, G. M., Butlin, R. K., & East, T. M. (1987). Testicular dysfunction in hybrids between parapatric subspecies of the grasshopper *Chorthippus parallelus*. *Biological Journal of the Linnean Society*, 31(1), 25–34. https://doi.org/10.1111/j.1095-8312.1987.tb01978.x

Hoang, D. T., Chernomor, O., von Haeseler, A., Minh, B. Q., & Vinh, L. S. (2018). UFBoot2: Improving the ultrafast bootstrap approximation. *Molecular Biology and Evolution*, 35(2), 518–522. https://doi.org/10.1093/molbev/msx281

Ivy-Ochs, S., Kerschner, H., Reuther, A., Preusser, F., Heine, K., Maisch, M., & Schlüchter, C. (2008). Chronology of the last glacial cycle in the European Alps. *Journal of Quaternary Science*, 23(6–7), 559–573. https://doi.org/10.1002/jqs.1202

Kalyaanamoorthy, S., Minh, B. Q., Wong, T. K. F., von Haeseler, A., & Jermiin, L. S. (2017). ModelFinder: Fast model selection for accurate phylogenetic estimates. *Nature Methods*, 14(6), 587–589. https://doi.org/10.1038/nmeth.4285

Kliman, R. M., Andolfatto, P., Coyne, J. A., Depaulis, F., Kreitman, M., Berry, A. J., & Hey, J. (2000). The Population genetics of the origin and divergence of the *Drosophila simulans* complex species. *Genetics*, 156(4), 1913–1931. https://doi.org/10.1093/genetics/156.4.1913

Korkmaz, E. M., Lunt, D. H., Çıplak, B., Değerli, N., & Başıbüyük, H. H. (2014). The contribution of Anatolia to European phylogeography: The centre of origin of the meadow grasshopper, *Chorthippus parallelus*. *Journal of Biogeography*, 41(9), 1793–1805. https://doi.org/10.1111/jbi.12332

Korneliussen, T. S., Albrechtsen, A., & Nielsen, R. (2014). ANGSD: Analysis of next generation sequencing data. *BMC Bioinformatics*, 15(1), 356. https://doi.org/10.1186/s12859-014-0356-4

Koschuh, A. (2008). Podismopsis styriaca nov. Sp. (orthoptera, Acridinae) Ein Endemit Im Ostalpenraum. Na.

Li, H., & Durbin, R. (2009). Fast and accurate short read alignment with Burrows-Wheeler transform. *Bioinformatics*, 25(14), 1754–1760. https://doi.org/10.1093/bioinformatics/btp324

Lohse, K., Nicholls, J. A., & Stone, G. N. (2011). Inferring the colonization of a mountain range—Refugia vs. Nunatak survival in high alpine ground beetles. *Molecular Ecology*, 20(2), 394–408. https://doi.org/10.1111/j.1365-294X.2010.04929.x

Lunt, D. H., Ibrahim, K. M., & Hewitt, G. M. (1998). MtDNA phylogeography and postglacial patterns of subdivision in the meadow grasshopper *Chorthippus parallelus*. *Heredity*, 80(5), 633–641. https://doi.org/10.1046/j.1365-2540.1998.00311.x

Masly, J. P., & Presgraves, D. C. (2007). High-resolution genome-wide dissection of the two rules of speciation in Drosophila. *PLoS Biology*, 5(9), e243. https://doi.org/10.1371/journal.pbio.0050243

Matute, D. R. (2010). Reinforcement can overcome gene flow during speciation in Drosophila. *Current Biology*, 20(24), 2229–2233. https://doi.org/10.1016/j.cub.2010.11.036

Matute, D. R., & Cooper, B. S. (2021). Comparative studies on speciation: 30 years since Coyne and Orr. *Evolution*, 75(4), 764–778. https://doi.org/10.1111/evo.14181

Mirarab, S., Reaz, R., Bayzid, M. S., Zimmermann, T., Swenson, M. S., & Warnow, T. (2014). ASTRAL: Genome-scale coalescent-based species tree estimation. *Bioinformatics*, 30(17), i541–i548. https://doi.org/10.1093/bioinformatics/btu462

Mirarab, S., & Warnow, T. (2015). ASTRAL-II: Coalescent-based species tree estimation with many hundreds of taxa and thousands of genes. *Bioinformatics*, 31(12), i44–i52. https://doi.org/10.1093/bioinformatics/btv234

Muller, H. (1942). Isolating mechanisms, evolution, and temperature. *Biology Symposium*, 6, 71–125.

Nachman, M. W., & Payseur, B. A. (2012). Recombination rate variation and speciation: Theoretical predictions and empirical results from rabbits and mice. *Philosophical Transactions of the Royal Society B: Biological Sciences*, 367(1587), 409–421.

Nadig, A. (1989). Eine aus den Alpen bisher unbekannte Untergattung in der Schweiz: Chrysochraon (Podismopsis) keisti sp. N. (saltatoria, Acrididae). *Mitteilungen Der Schweizerischen Entomologischen Gesellschaft*, 62(1–2), 79–86.

Naisbit, R. E., Jiggins, C. D., & Mallet, J. (2001). Disruptive sexual selection against hybrids contributes to speciation between Heliconius cydno and Heliconius melpomene. *Proceedings of the Royal Society of London. Series B: Biological Sciences*, 268(1478), 1849–1854. https://doi.org/10.1098/rspb.2001.1753

Nei, M., & Li, W.-H. (1979). Mathematical model for studying genetic variation in terms of restriction endonucleases. *Proceedings of the National Academy of Sciences*, 76(10), 5269–5273. https://doi.org/10.1073/pnas.76.10.5269

Nguyen, L.-T., Schmidt, H. A., von Haeseler, A., & Minh, B. Q. (2015). IQ-TREE: A fast and effective stochastic algorithm for estimating maximum-likelihood phylogenies. *Molecular Biology and Evolution*, 32(1), 268–274. https://doi.org/10.1093/molbev/msu300

Nolen, Z. J., Yildirim, B., Irisarri, I., Liu, S., Groot Crego, C., Amby, D. B., & Pereira, R. J. (2020). Historical isolation facilitates species radiation by sexual selection: Insights from *Chorthippus* grasshoppers. *Molecular Ecology*, 29(24), 4985–5002. https://doi.org/10.1111/mec.15695

Nürnberger, B., Lohse, K., Fijarczyk, A., Szymura, J. M., & Blaxter, M. L. (2016). Para-allopatry in hybridizing fire-bellied toads (*Bombina bombina* and *B. variegata*): Inference from transcriptome-wide coalescence analyses. *Evolution*, 70(8), 1803–1818.

Palacios, D., de Andrés, N., Gómez-Ortiz, A., & García-Ruiz, J. M. (2017). Evidence of glacial activity during the Oldest Dryas in the mountains of Spain. *Geological Society, London, Special Publications*, 433(1), 87–110. https://doi.org/10.1144/SP433.10

Papadopoulou, A., Anastasiou, I., & Vogler, A. P. (2010). Revisiting the insect mitochondrial molecular clock: The mid-Aegean trench calibration. *Molecular Biology and Evolution*, 27(7), 1659–1672. https://doi.org/10.1093/molbev/msq051

Paradis, E., & Schliep, K. (2019). ape 5.0: An environment for modern phylogenetics and evolutionary analyses in R. *Bioinformatics*, 35(3), 526–528. https://doi.org/10.1093/bioinformatics/bty633

Payseur, B. A., Presgraves, D. C., & Filatov, D. A. (2018). Sex chromosomes and speciation. *Molecular Ecology*, 27(19), 3745.

Payseur, B. A., & Rieseberg, L. H. (2016). A genomic perspective on hybridization and speciation. *Molecular Ecology*, 25(11), 2337–2360. https://doi.org/10.1111/mec.13557

Pereira, R. J., Ruiz-Ruano, F. J., Thomas, C. J. E., Pérez-Ruiz, M., Jiménez-Bartolomé, M., Liu, S., & Bella, J. L. (2021). Mind the numt: Finding informative mitochondrial markers in a giant grasshopper genome. *Journal of Zoological Systematics and Evolutionary Research*, 59(3), 635–645. https://doi.org/10.1111/jzs.12446

Pfennig, D. W., & Pfennig, K. S. (2012). *Evolution's wedge: Competition and the origins of diversity*. University of California Press. https://doi.org/10.1525/california/9780520274181.001.0001

Phifer-Rixey, M., Harr, B., & Hey, J. (2020). Further resolution of the house mouse (Mus musculus) phylogeny by integration over isolation-with-migration histories. *BMC Evolutionary Biology*, 20(1), 120. https://doi.org/10.1186/s12862-020-01666-9

Poelstra, J. W., Vijay, N., Bossu, C. M., Lantz, H., Ryll, B., Müller, I., Baglione, V., Unneberg, P., Wikelski, M., Grabherr, M. G., & Wolf, J. B. W. (2014). The genomic landscape underlying phenotypic integrity in the face of gene flow in crows. *Science*, *344*(6190), 1410–1414. https://doi.org/10.1126/science.1253226

Pollard, D. A., Iyer, V. N., Moses, A. M., & Eisen, M. B. (2006). Widespread discordance of gene trees with species tree in Drosophila: Evidence for incomplete lineage sorting. *PLoS Genetics*, *2*(10), e173. https://doi.org/10.1371/journal.pgen.0020173

Presgraves, D. C. (2010). The molecular evolutionary basis of species formation. *Nature Reviews Genetics*, *11*(3), 175–180. https://doi.org/10.1038/nrg2718

Presgraves, D. C. (2018). Evaluating genomic signatures of "the large X-effect" during complex speciation. *Molecular Ecology*, *27*(19), 3822–3830. https://doi.org/10.1111/mec.14777

Presgraves, D. C., & Meiklejohn, C. D. (2021). Hybrid sterility, genetic conflict and complex speciation: Lessons from the *Drosophila simulans* clade species. *Frontiers in Genetics*, *12*, e669045. https://doi.org/10.3389/fgene.2021.669045

Rafati, N., Blanco-Aguiar, J. A., Rubin, C. J., Sayyab, S., Sabatino, S. J., Afonso, S., Feng, C., Alves, P. C., Villafuerte, R., Ferrand, N., Andersson, L., & Carneiro, M. (2018). A genomic map of clinal variation across the European rabbit hybrid zone. *Molecular Ecology*, *27*(6), 1457–1478. https://doi.org/10.1111/mec.14494

Rambaut, A., Drummond, A. J., Xie, D., Baele, G., & Suchard, M. A. (2018). Posterior summarization in Bayesian phylogenetics using tracer 1.7. *Systematic Biology*, *67*(5), 901–904. https://doi.org/10.1093/sysbio/syy032

Ravinet, M., Westram, A., Johannesson, K., Butlin, R. K., André, C., & Panova, M. (2016). Shared and nonshared genomic divergence in parallel ecotypes of *Littorina saxatilis* at a local scale. *Molecular Ecology*, *25*(1), 287–305. https://doi.org/10.1111/mec.13332

Reynolds, J., Weir, B. S., & Cockerham, C. C. (1983). Estimation of the coancestry coefficient: Basis for a short-term genetic distance. *Genetics*, *105*(3), 767–779. https://doi.org/10.1093/genetics/105.3.767

Riesch, R., Muschick, M., Lindtke, D., Villoutreix, R., Comeault, A. A., Farkas, T. E., Lucek, K., Hellen, E., Soria-Carrasco, V., Dennis, S. R., de Carvalho, C. F., Safran, R. J., Sandoval, C. P., Feder, J., Gries, R., Crespi, B. J., Gries, G., Gompert, Z., & Nosil, P. (2017). Transitions between phases of genomic differentiation during stick-insect speciation. *Nature Ecology & Evolution*, *1*(4), 1–13. https://doi.org/10.1038/s41559-017-0082

Rieseberg, L. H., Baird, S. J., & Gardner, K. A. (2000). Hybridization, introgression, and linkage evolution. *Plant Molecular Evolution*, *42*, 205–224.

Ritchie, M. G., Butlin, R. K., & Hewitt, G. M. (1989). Assortative mating across a hybrid zone in *Chorthippus parallelus* (Orthoptera: Acrididae). *Journal of Evolutionary Biology*, *2*(5), 339–352. https://doi.org/10.1046/j.1420-9101.1989.2050339.x

Ritchie, M. G., Butlin, R. K., & Hewitt, G. M. (1992). Fitness consequences of potential assortative mating inside and outside a hybrid zone in *Chorthippus parallelus* (Orthoptera: Acrididae): Implications for reinforcement and sexual selection theory. *Biological Journal of the Linnean Society*, *45*(3), 219–234. https://doi.org/10.1111/j.1095-8312.1992.tb00641.x

Schubert, M., Ermini, L., Sarkissian, C. D., Jónsson, H., Ginolhac, A., Schaefer, R., Martin, M. D., Fernández, R., Kircher, M., McCue, M., Willerslev, E., & Orlando, L. (2014). Characterization of ancient and modern genomes by SNP detection and phylogenomic and metagenomic analysis using PALEOMIX. *Nature Protocols*, *9*(5), 1056–1082. https://doi.org/10.1038/nprot.2014.063

Schubert, M., Lindgreen, S., & Orlando, L. (2016). AdapterRemoval v2: Rapid adapter trimming, identification, and read merging. *BMC Research Notes*, *9*(1), 88. https://doi.org/10.1186/s13104-016-1900-2

Semenov, G. A., Linck, E., Enbody, E. D., Harris, R. B., Khaydarov, D. R., Alström, P., Andersson, L., & Taylor, S. A. (2021). Asymmetric introgression reveals the genetic architecture of a plumage trait. *Nature Communications*, *12*(1), 1019. https://doi.org/10.1038/s41467-021-21340-y

Serrano, L., de la Vega, C. G., Bella, J. L., López-Fernández, C., Hewitt, G. M., & Gosálvez, J. (1996). A hybrid zone between two subspecies of *Chorthippus parallelus*. X-chromosome variation through a contact zone. *Journal of Evolutionary Biology*, *9*(2), 173–184. https://doi.org/10.1046/j.1420-9101.1996.9020173.x

Servedio, M. R., & Noor, M. A. F. (2003). The role of reinforcement in speciation: Theory and data. *Annual Review of Ecology, Evolution, and Systematics*, *34*(1), 339–364. https://doi.org/10.1146/annurev.ecolsys.34.011802.132412

Shen, L. (2021). GeneOverlap: Test and visualize gene overlaps. R package version 1.30.0. http://shenlabsinai.github.io/shenlab-sinai/

Shuker, D. M., Underwood, K., King, T. M., & Butlin, R. K. (2005). Patterns of male sterility in a grasshopper hybrid zone imply accumulation of hybrid incompatibilities without selection. *Proceedings of the Royal Society B: Biological Sciences*, *272*(1580), 2491–2497.

Skotte, L., Korneliussen, T. S., & Albrechtsen, A. (2013). Estimating individual admixture proportions from next generation sequencing data. *Genetics*, *195*(3), 693–702. https://doi.org/10.1534/genetics.113.154138

Slatkin, M. (1985). Gene flow in natural populations. *Annual Review of Ecology and Systematics*, *16*(1), 393–430. https://doi.org/10.1146/annurev.es.16.110185.002141

Sobel, J. M., Chen, G. F., Watt, L. R., & Schemske, D. W. (2010). The biology of speciation. *Evolution*, *64*(2), 295–315. https://doi.org/10.1111/j.1558-5646.2009.00877.x

Song, H., Mariño-Pérez, R., Woller, D. A., & Cigliano, M. M. (2018). Evolution, diversification, and biogeography of grasshoppers (Orthoptera: Acrididae). *Insect Systematics and Diversity*, *2*(4), 3. https://doi.org/10.1093/isd/ixy008

Soraggi, S., Wiuf, C., & Albrechtsen, A. (2018). Powerful inference with the D-statistic on low-coverage whole-genome data. *G3: Genes, Genomes, Genetics*, *8*(2), 551–566. https://doi.org/10.1534/g3.117.300192

Stehlik, I., Blattner, F., Holderegger, R., & Bachmann, K. (2002). Nunatak survival of the high Alpine plant *Eritrichium nanum* (L.) Gaudin in the central Alps during the ice ages. *Molecular Ecology*, *11*(10), 2027–2036.

Stern, D. L., & Orgogozo, V. (2009). Is genetic evolution predictable? *Science*, *323*(5915), 746–751.

Strimmer, K., & von Haeseler, A. (1997). Likelihood-mapping: A simple method to visualize phylogenetic content of a sequence alignment. *Proceedings of the National Academy of Sciences*, *94*(13), 6815–6819. https://doi.org/10.1073/pnas.94.13.6815

Suchard, M. A., Lemey, P., Baele, G., Ayres, D. L., Drummond, A. J., & Rambaut, A. (2018). Bayesian phylogenetic and phylodynamic data integration using BEAST 1.10. *Virus Evolution*, *4*(1), vey016. https://doi.org/10.1093/ve/vey016

Tajima, F. (1989). Statistical method for testing the neutral mutation hypothesis by DNA polymorphism. *Genetics*, *123*(3), 585–595. https://doi.org/10.1093/genetics/123.3.585

Tamura, K., Dudley, J., Nei, M., & Kumar, S. (2007). MEGA4: Molecular evolutionary genetics analysis (MEGA) software version 4.0. *Molecular Biology and Evolution*, *24*(8), 1596–1599. https://doi.org/10.1093/molbev/msm092

Teeter, K. C., Payseur, B. A., Harris, L. W., Bakewell, M. A., Thibodeau, L. M., O'Brien, J. E., Krenz, J. G., Sans-Fuentes, M. A., Nachman, M. W., & Tucker, P. K. (2007). Genome-wide patterns of gene flow across a house mouse hybrid zone. *Genome Research*, *18*(1), 67–76. https://doi.org/10.1101/gr.6757907

Thompson, K. A., Peichel, C. L., Rennison, D. J., McGee, M. D., Albert, A. Y. K., Vines, T. H., Greenwood, A. K., Wark, A. R., Brandvain, Y.,

Schumer, M., & Schluter, D. (2022). Analysis of ancestry heterozygosity suggests that hybrid incompatibilities in threespine stickleback are environment dependent. *PLoS Biology*, *20*(1), e3001469. https://doi.org/10.1371/journal.pbio.3001469

Turner, L. M., & Harr, B. (2014). Genome-wide mapping in a house mouse hybrid zone reveals hybrid sterility loci and Dobzhansky-Muller interactions. *eLife*, *3*, e02504. https://doi.org/10.7554/eLife.02504

Virdee, S. R., & Hewitt, G. M. (1992). Postzygotic isolation and Haldane's rule in a grasshopper. *Heredity*, *69*(6), 527–538. https://doi.org/10.1038/hdy.1992.168

Virdee, S. R., & Hewitt, G. M. (1994). Clines for hybrid dysfunction in a grasshopper hybrid zone. *Evolution*, *48*(2), 392–407. https://doi.org/10.1111/j.1558-5646.1994.tb01319.x

Wachter, G. A., Arthofer, W., Dejaco, T., Rinnhofer, L. J., Steiner, F. M., & Schlick-Steiner, B. C. (2012). Pleistocene survival on central Alpine nunataks: Genetic evidence from the jumping bristletail *Machilis pallida*. *Molecular Ecology*, *21*(20), 4983–4995.

Wang, R. L., & Hey, J. (1996). The Speciation History of *Drosophila pseudoobscura* and close relatives: Inferences from DNA sequence variation at the period locus. *Genetics*, *144*(3), 1113–1126.

Watterson, G. A. (1975). On the number of segregating sites in genetical models without recombination. *Theoretical Population Biology*, *7*(2), 256–276. https://doi.org/10.1016/0040-5809(75)90020-9

Westram, A. M., Faria, R., Johannesson, K., & Butlin, R. K. (2021). Using replicate hybrid zones to understand the genomic basis of adaptive divergence. *Molecular Ecology*, *30*(15), 3797–3814. https://doi.org/10.1111/mec.15861

Zabal-Aguirre, M., Arroyo, F., & Bella, J. (2010). Distribution of Wolbachia infection in *Chorthippus parallelus* populations within and beyond a Pyrenean hybrid zone. *Heredity*, *104*(2), 174–184. https://doi.org/10.1038/hdy.2009.106

Zieliński, P., Dudek, K., Arntzen, J. W., Palomar, G., Niedzicka, M., Fijarczyk, A., Liana, M., Cogălniceanu, D., & Babik, W. (2019). Differential introgression across newt hybrid zones: Evidence from replicated transects. *Molecular Ecology*, *28*(21), 4811–4824. https://doi.org/10.1111/mec.15251

SUPPORTING INFORMATION

Additional supporting information may be found in the online version of the article at the publisher's website.